Available online www.jocpr.com

Journal of Chemical and Pharmaceutical Research, 2017, 9(6):262-280

Review Article

ISSN : 0975-7384
CODEN(USA) : JCPRC5

Experimental and Theoretical Investigation of the Molecular and Electronic Structure of 3-Acetoxy-2-Methylbenzoic Acid using Quantum Chemical Computational Calculations

K Karthikeyan[1,2], C Arunagiri[1*], A Subashini[3], AG Anitha[1,4] and S Selvakumar[1]

[1]Department of Physics, Government Arts College, Ariyalur, Tamilnadu, India
[2]Department of Physics, Saranathan College of Engineering, Tiruchirappalli, Tamilnadu India
[3]Department of Chemistry, Seethalakshmi Ramaswami College,Tiruchirappalli, Tamilnadu, India
[4] Department of Physics, Seethalakshmi Ramaswami College, Tiruchirappalli, Tamilnadu, India

---

ABSTRACT

In this work, experimental and theoretical study on the molecular structure of 3-acetoxy-2-methyl benzoic acid (3A2MBA) is performed based on the quantum mechanical approach by density functional theory (DFT) calculations. The optimized geometrical parameters were done by DFT using the B3LYP method show good agreement with experimental X-ray data. The vibrational harmonic frequencies were scaled using scale factors, yielding a good agreement between the experimentally recorded and the theoretically calculated values with the aid of a calculation of the Total energy distribution (TED). The population of electrons in core, valance and Rydberg sub-shells have been predicted. The natural hybrid atomic orbital studies enhance us to know about the type of orbitals and its percentage of s-type and p-type character. The intra molecular charge transfers occurring in the molecule have been analyzed by NBO analysis. The study is extended to HOMO–LUMO analysis, ionization potential, electron affinity, electrophilicity index, chemical potential, electro negativity, softness, hardness and thermodynamic properties of 3A2MBA.

Keywords: 3A2MBA; DFT; FT-IR; FT-Raman; HOMO; LUMO

INTRODUCTION

Benzoic acid is a compound that has an elegant simplicity to its molecular structure, but its derivatives display an enormous complexity and diversity of molecular structures. The derivatives of benzoic acid have been the subject of investigation as this form an essential component of the vitamin B-complex. Benzoic acid occurs widely in plants and animal tissues along with vitamin B-complex and is used to raise the salicylate level in blood. It is used as antifungal agents for superficial fungus infection of skin. Together with salicylic acids in Whitefield's ointments, which is used for the treatment of fungal skin diseases such as tinea, ring worm in dogs and other species[1]. Benzoic acid and its sodium salt (sodium benzoate) are the most common, safe, food preservatives and antimicrobial agents. Recognizing the commercial availability and low cost of benzoic acid and sodium benzoate, they are found to be attractive candidates to be incorporated into coatings as environmentally benign alternatives [2,3]. The crystal structures of unsubstituted benzoic acid using X-ray diffraction [4,5] as well as the crystal structures of benzoic acid derivatives bearing a halogen atom in an ortho position to the carboxylic acid group are apparent in the literature [6-8]. Crystal structures of 2-acetoxy-3-methylbenzoic acid (3-methyl aspirin) and 2-acetoxy-6-methylbenzoic acid (6-methyl aspirin) have already been reported in the literature [9,10]. Aspirin is a unique drug as it is effective against pain, it has anti-pyretic and anti-inflammatory properties, and it is widely used during heart attacks or strokes. A series of water-soluble (benzoyloxy) methyl esters of acetylsalicylic acid (ASA) as pro drugs was synthesized and evaluated by Rolando et al. [11]. Ulla Derthasching et al. have investigated the effects of aspirin on platelet function and

coagulation in human endotoxemia [12]. Investigations on the structure and fundamental vibrations of benzoic acid and its derivatives are still being carried out, increasingly. Vibrational spectra of benzoic acid and substituted benzoic acids have been studied by various workers [13-18]. Amalanathan et al. studied the infrared absorption spectra of 3,5-dinitrobenzoic acid have been recorded in the solid phase [19]. The stokes and anti stokes laser Raman spectra of 2,3,5-triiodobenzoic acid have been studied [15]. The molecule 3-acetoxy-2-methylbenzoic acid is a light yellow crystalline solid; it is used as an intermediate in the preparation of small-sized HIV protease inhibitors [20]. For this reason, we are interested in this class of compounds as potential agents in other diseases. The theoretical calculation of the title molecule is described herein. Previously we have reported crystal structure of 3-acetoxy-2-methylbenzoic acid [21]. Literature survey reveals that to the best of our knowledge no vibrational spectroscopic analysis of 3-acetoxy-2- methyl benzoic acid by the quantum mechanical DFT method have been reported so far. Therefore, the present investigation was undertaken to study the vibrational spectra of this molecule completely and to identify the various normal modes with greater wavenumber accuracy. The theoretical Density Functional Theory (DFT) studies give information regarding the structural parameters, the functional groups, orbital interactions and vibrational frequencies. DFT have evolved to be a powerful and reliable tool for the determination of various molecular properties. B3LYP functional have provided an excellent compromise between accuracy and computational efficiency of vibrational spectra for large and medium size molecule [22-25]. For this reason, by employing the DFT (B3LYP) method, we have calculated the geometric parameters and vibrational spectra of 3-acetoxy-2-methylbenzoic acid in the ground state and compared with the experimental vibrational frequencies. Vibrational assignments were carried out on the basis of total energy distributions (TED) and experimental data. In addition, the ionization potential, electron affinity, electrophilicity index, chemical potential, electronegativity, softness, hardness, HOMO – LUMO energy, natural population analysis, natural orbital analysis and thermodynamic properties calculations were carried out calculations were carried out using B3LYP with 6-31+G(d,p) and 6-311++G(d,p) method. These calculations were expected to provide new insight in to the vibrational spectra and molecular parameters.

EXPERIMENTAL SECTION

The FT-IR spectrum of the title molecule was recorded in the region 4000-400 cm^{-1} on a BRUKER IFS 66V spectrophotometer using the KBr pellet technique. The spectrum was recorded at room temperature, with a scanning speed of 10 cm^{-1} per minute and at the spectral resolution of 2.0 cm^{-1}. The FT-Raman spectrum of this molecule was also recorded in the region 3500-50 cm^{-1} with BRUKER RFS 27 Raman module equipped with Nd:YAG laser source operating at 1064 nm line width 100 mW power. The spectrum was recorded with scanning speed of 50 cm^{-1} min^{-1} of spectral width 4 cm^{-1}. The reported wave numbers are believed to be accurate within ±1 cm^{-1}.

Computational Methods

Quantum chemical density functional theory calculations were carried out with the 2009 version of the Gaussian program package [26] using B3LYP functions [27,28] combined with the standard 6-31+G(d,p) and 6-311++G(d,p) basis sets (referred to as small and large basis sets, respectively). The Cartesian representation of the theoretical force constants has been computed at the optimized geometry by assuming C_s point group symmetry. The optimized geometrical parameters, fundamental vibrational frequencies, IR intensity, Raman activity, reduced mass, force constant and thermodynamic parameters were calculated. From the intensity theory of Raman scattering [29] the relative Raman intensities (*Ii*) and Raman activities (Si) were calculated:

$$I_i = \frac{f\left(\nu_0 - \nu_i\right)^4 S_i}{\nu_i\left(1 - \exp\left(-\frac{hc\nu_i}{kT}\right)\right)} \qquad \text{... (1)}$$

Where, ν_0 is the exciting wavenumber; ν_i the vibrational wavenumber of the normal mode; *h*, *c* and *k* are the universal constants, and *f* is the suitably chosen common normalization factor for all the peak intensities. Scaling of the force field was performed according to the SQM procedure [30,31] using selective scaling in the natural internal coordinate representation [32]. Transformation of the force field and the subsequent normal coordinate analysis (NCA) including the least squares refinement of the scaling factors, calculation of total energy distribution (TED) were done on a PC with the MOLVIB program (version 7.0-G77) written by Sundius [33-35].

RESULTS AND DISCUSSION

Geometrical Parameters

The molecular structure of title molecule belongs to C_s point group symmetry. The optimized molecular structure of title molecule is obtained from Gaussian 09W as shown in Figure 1. The most optimized structural

parameters of 3-acetoxy-2-methylbenzoic acid are calculated by B3LYP level with 6-31+G(d,p) and 6-311++G(d,p) basis sets and presented in Table 1. The results are compared with the experimental X-ray diffraction data [21]. From the single crystal XRD data, the title molecule has the cell dimensions are a = 7.754 Å; b = 11.346 Å; c = 21.187 Å; α = γ = 90°; β = 95° have been already reported [21]. The values of all the bond lengths and bond angles have small deviations with the experimental (XRD) and theoretical results (which are calculated by B3LYP/6-31+G(d,p) and 6-311++G(d,p) basis sets). This is due to the theoretical calculations are performed (for an isolated molecule) in gaseous phase whereas the experimental results are obtained from solid state. From the crystal data of title molecule, the C11-H12, C11-H13, C11-H14, C18-H19, C18-H20, C18-H21, C4-H22, C5-H23 and C6-H24 bond lengths are shorter than those of the calculated B3LYP values and this is caused by the inter molecular hydrogen bonding in crystalline state. The calculated and experimental C-O group bond distances are almost equal in C7-O8, C7-O9, C3-O15, C16-O15 and O17-C16. Electron donating groups are generally ortho/para directors which electron withdrawing groups are meta directors with the exception of halogens (X = Cl, F, I, Br). When a functional –COOH group bonded to a benzene ring, the bond angle around C1 atom (C6-C1-C2) is 120.8° which confirms the tetrahedral arrangement of C1 atom. With the electron donating substituents (–CH_3 group) on the benzene ring and the bond angle smaller than 120° (C1-C2-C3) at the point of substitution bond angle larger than 120° at the meta position where –$OCOCH_3$ is attached (C4-C3-C2 = 128.8°). Due to the electron withdrawing nature of the substituents, it is observed that in title molecule the bond angle at the point of substitution C2-C3-O15 is equal values 119.30° and 119.84° in B3LYP while the bond angle is 118.6° by experiment, as shown in Table 1. The calculated bond angles using both basis sets for C2-C3-C4, C3-C4-C5, C4-C5-C6, C4-C5-H15, C6-C5-H15, C5-C6-C7, C5-C6-H16 and C7-C6-H16 are in good agreement with the experimental ones and the small variation in remaining bond angles depends on the electro negativity of the central atom, the presence of lone pair of electrons and the conjugation of the double bonds.

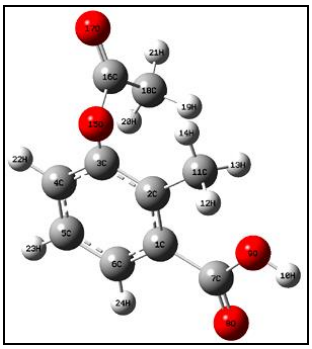

Figure 1: Molecular structure and atomic labelling of 3A2MBA

Vibrational Spectra

In our present study, we have performed a frequency calculation analysis to obtain the spectroscopic signature of 3-acetoxy-2-methylbenzoic acid (3A2MBA). The molecule 3A2MBA has an orthorhombic structure of Pbca space group and Cs point group symmetry. The vibrational spectral analysis of the molecule 3A2MBA is done based on normal coordinate analysis followed by scaled quantum mechanical force field calculations. The 3A2MBA molecule consists of 24 atoms therefore they have 66 vibrational normal modes. Out of 66 modes of fundamental vibrations 45 modes should be in-plane symmetric (A') and 21 modes out-of-plane symmetric (A") with respect to the reflection on the symmetry plane. All the frequencies are assigned in terms of fundamental, overtone and combination bands. The recorded (FT-IR and FT-Raman) and calculated vibrational wavenumbers along with their relative intensities and probable assignments with TED of 3A2MBA molecule are given in Table 2. The theoretical spectra were obtained from the B3LYP/6-31+G (d,p) and 6-311++G(d,p) method using Lorentzian band shape with band width on half-height 10 cm^{-1}. This reveals good correspondence between theory and experiment in main spectral features. The experimental spectra are shown in Figures 2 and 3, respectively. The computed vibrational wavenumbers and the atomic displacements corresponding to the different normal modes are used for identifying the vibrational modes unambiguously. In order to simulate H bonding through COOH group we also calculated the vibrational wavenumbers of 3A2MBA molecule. The calculated wavenumbers are usually higher than the corresponding experimental quantities, due to the combination of electron correlation effects and basis sets deficiencies. After applying, the different scaling factors, the theoretical wavenumbers are in good agreement with experimental wavenumbers [26].

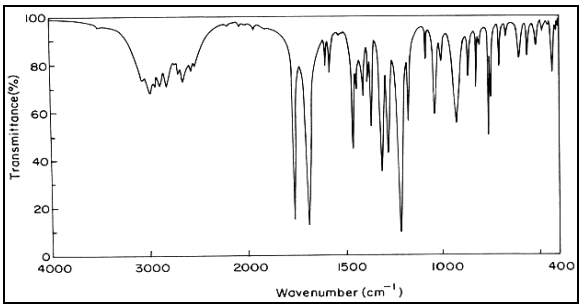

Figure 2: FT-IR spectrum of 3A2MBA

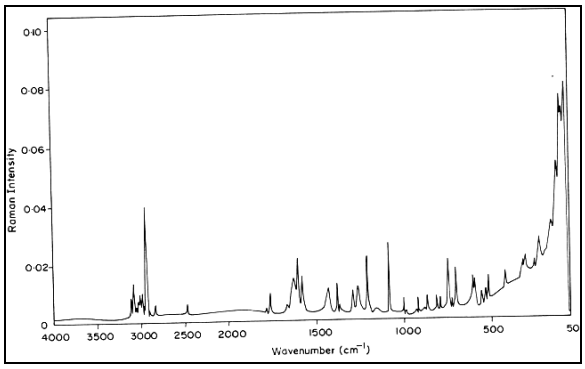

Figure 3: FT-Raman spectrum of 3A2MBA

Carboxylic Acid (–COOH) Group Vibrations

The vibrational analysis of carboxylic acid (–COOH) group is made on the basis of carbonyl group and hydroxyl group vibrations. The carboxylic group is substituted at the first position in benzene ring of the 3A2MBA molecule. The vibrational analysis of –COOH group is significant because of the activity of the title molecule which is mainly due to either the presence of this moiety or a group that is easily converted to it within the plant tissues [36] and which is made on the basis of carbonyl group and the hydroxyl group. The vibrational bands of the –COOH groups of 3A2MBA contain the C–O, C=O and O–H vibrational modes. C=O stretching band appears strongly in the region 1870–1540 cm^{-1} in which the position of C=O stretching band depends on the physical state, electronic and mass effects of neighboring substituents, conjugations, intra molecular and intermolecular hydrogen bonding [37-44]. The O–H group stretching vibrations are likely to be most sensitive to the environment, so they show pronounced shifts in the spectra of the hydrogen bonded species. A free hydroxyl group or a non-hydrogen bonded hydroxyl group absorbs in the range 3700–3500 cm^{-1}, whereas the existence of intermolecular hydrogen bond formation can lower the O−H stretching frequency to the 3550–3200 cm^{-1} region with increase in intensity and breath [39-42]. In the present investigation, the stretching vibration of O−H group is assigned as a very weak band observed at 3317 cm^{-1} in the recorded FT-IR spectrum. The O–H stretching modes are found as 3329 and 3322 cm^{-1} by B3LYP calculation levels, as given in Table 2. The theoretically computed scaled frequency for O−H vibration by B3LYP/6-311++G(d,p) method shows excellent agreement with recorded spectrum as well as the literature data and also find support from TED values of 100%. The lower stretching frequency observed in 3A2MBA compared with the free O–H group stretching signifies that there is a possibility of intermolecular hydrogen bonding in 3A2MBA, between the hydroxyl group and carbonyl group of molecule. The O−H in-plane bending vibrations occur in the general region of 1420-1330 cm^{-1} and are not much affected due to hydrogen bonding unlike the stretching and out-of-plane bending frequencies. The in-plane banding mode of hydroxyl group was recorded at 1375 cm^{-1} in FT-Raman spectrum and computed at 1384 and 1381 cm^{-1} with 53% value of TED contribution for title molecule. They show good agreement with the theoretically computed B3LYP/6-311++G (d,p) method. The O−H out-of-plane bending vibrations appear in the region 320–290 cm^{-1} for free O–H and in the region 710–570 cm^{-1} for associated benzoic acids [43]. The carboxylic acids show out-of-plane bending band of O–H vibration occurred at 704cm^{-1} in FT-Raman spectrum of 3A2MBA. The TED calculations show that the hydroxyl stretching vibrational mode is very pure. But the in-plane bending vibration of the hydroxyl group is overlapped with the other vibrations. The band due to the free hydroxyl group is sharp and its intensity increases. The C=O stretching mode is the strongest bands in the infrared and appears with diminished intensity weak bands in the Raman spectra (less polarizability resulting due to highly dipolar carbonyl bond) around 1800–1650 cm^{-1} in aromatic compounds is the most salient feature of the presence of carbonyl group and are due to the C=O stretching motions [43,44]. The wavenumber of the C=O stretch due to carbonyl group mainly depends on the bond strength, which in turn depends upon inductive,

conjugative, steric effects and the lone pair of electrons on oxygen. Hence the weak FT-Raman band observed at 1769 cm^{-1} is assigned to the C=O stretching band of 3A2MBA molecule. As indicated by TED, this mode involves exact contribution of 89% suggesting that it is a pure stretching mode. The similar vibrations are calculated at 1781 and 1778 cm^{-1} by DFT-B3LYP/6-31+G (d,p) and 6-311++G (d,p) method. However, the computed scaled values observed at 1776 and 1773 cm^{-1} of C=O stretching vibrations shows better agreement with the experimental data. However, it is known that C=O stretching and O− H bending modes are not independent vibrational modes because they coupled with the vibrations of adjacent groups. The C–O stretching band is occurs at 1450-1150 cm^{-1} regions depending on whether monomer or other hydrogen bonded species are present. Generally the C–O stretching mode appears at lower frequency than the C–OH bending mode. However, these bands overlap with other bands that are due to aromatic or aliphatic chain vibrations. Based on the above information, the FT-Raman band observed at 1262 cm^{-1} has been assigned to C–O stretching vibration for 3A2MBA. In addition carboxylic acids also show C=O and C–O in-plane and out-of-plane bending vibrations are also listed in Table 2.

C–H Vibrations

In general, the aromatic structure shows presence of C-H stretching vibration in the band region 3100–3000 cm^{-1} [45]. Bayari et al. have reported C–H stretching frequencies in the range of 3125–3000 cm^{-1} [46]. In the present investigation, three weak bands observed in FT-Raman spectrum at 3125, 3100 and 3075 cm^{-1} are assigned to C4–H22, C5–H23 and C6–H24 stretching vibrations. The theoretically calculated wave numbers agree closely with the experimental spectral values as seen in Table 2. These assignments are well supported by calculated TED values. All bands have weak intensities and were obtained in the expected region. As expected, these three modes are pure stretching modes as it is evident from TED column. The C–H in-plane bending vibrations are assigned in the region 1300–1000 cm^{-1} [35]. For this compound, the C–H in-plane bending vibrations were observed at 1070, 1023 and 1011 cm^{-1} as strong and medium strong in FT-IR spectrum. The theoretically scaled vibrations by B3LYP/6-31+G(d,p) and 6-311++G(d,p) levels also shows good agreement with the experimentally recorded data. The C-H out-of-plane bending vibration appears within the region 1000-700 cm^{-1} [35]. The weak vibrations were identified at 776, 764 in FT-IR and 781 cm^{-1} in FT-Raman, and they are assigned to C-H out-of-plane bending vibrations for title molecule. These modes were computed at 803, 777, 730 cm^{-1} (unscaled)/ 766, 735, 713 cm^{-1} (scaled) and 801, 732, 778 cm^{-1} (unscaled) /764, 736, 711 cm^{-1} (scaled) by the B3LYP with 6-31+G (d,p) and 6-311++G (d,p) method. The C-H out-of-plane bending vibrations are also lie within the characteristic region and after scaling procedure, the theoretically scaled C-H vibrations are found to be in good agreement with the experimental values and literature [47]. The change in the frequencies of these deformations from the values in 3A2MBA is determined mainly by the relative position of the substituent and is almost independent of their nature.

C–C Vibrations

Vibrations of phenyl ring have been comprehensively studied according to Wilson's numbering convention [48]. The phenyl ring vibrational modes of title molecule have been analyzed based on the vibrational spectra of previously published vibrations of the benzene molecule is helpful in the identification of the phenyl ring modes [49-52]. The C–C ring stretching vibrations are very prominent, as the double bond is in conjugation with the ring, in the vibrational spectra of benzene and its derivatives [48]. The C–C stretching vibrations of the phenyl group are expected in the range 1650–1200 cm^{-1} [48]. In general, the five bands of variable intensity observed at 1625–1590, 1590-1575, 1540–1470, 1465–1430 and 1380–1280 cm^{-1} have been already reported by Varsanyi [44]. In the present work, the FT-IR and FT-Raman spectra bands of variable intensity observed at 1623(w), 1588(w), 1482(s), 1129(s) cm^{-1} and 1638(mw), 1602(ms), 1576(mw), 1087(s), 807(w) cm^{-1} have been assigned to C–C stretching vibrations in 3A2MBA. The theoretically computed (scaled) values at 1645, 1627, 1608, 1592, 1581, 1487, 1134, 1092 and 771 cm^{-1} by the B3LYP/6-311++G (d,p) method show an excellent agreement with experimental values. The C–C–C in-plane and out-of-plane bending vibrations are also calculated and the correlation between the experimental and theoretical values are observed as shown in Table 2. In lower frequency region C–C stretching and bending vibrations modes mixed with other vibrational modes and with small amount contributions were assigned based on TED results. From TED results, the most of these modes were assigned as pure vibrations. All the bands lie in the expected range to literature values. These observed frequencies show that, the substitutions in the ring to some extend affect the ring modes of vibrations. The comparison of the theoretically computed values were very good in agreement by B3LYP/6-311++G (d,p) method.

Table 1: Calculated optimized geometrical parameters of 3A2MBA

Bond lengths (Å)	Value (Å)			Bond angles (o)	Value (°)			Dihedral angles (o)	Value (°)		
	[a]Expt.	B3LYP			[a]Expt.	B3LYP			[a]Expt.	B3LYP	
		6-31+G(d,p)	6-311++G(d,p)			6-31+G(d,p)	6-311++G(d,p)			6-31+G(d,p)	6-311++G(d,p)
C1-C2	1.397	1.419	1.415	C2-C1-C6	120	120.84	120.42	C6-C1-C2-C3	0.1	-2	-2.1
C1-C6	1.384	1.405	1.401	C2-C1-C7	122.1	124.97	124.85	C6-C1-C2-C11	-179.8	176.6	176.1
C1-C7	1.462	1.496	1.496	C6-C1-C7	118	114.2	114.33	C7-C1-C2-C3	179.7	178.1	177.9
C2-C3	1.387	1.407	1.404	C1-C2-C3	116.2	116.2	116.31	C7-C1-C2-C11	-0.2	-3.2	-3.7
C2-C11	1.49	1.512	1.51	C1-C2-C11	124.4	124.72	124.62	C2-C1-C6-C5	0.4	0.6	0.8
C3-C4	1.374	1.394	1.391	C3-C2-C11	119.5	119.07	119.04	C2-C1-C6-H24	-	-179	-178.7
C3-O15	1.397	1.397	1.395	C2-C3-C4	123.6	123.04	122.34	C7-C1-C6-C5	-179.3	-179.4	-179.2
C4-C5	1.363	1.393	1.39	C2-C3-015	118.6	119.3	119.84	C7-C1-C6-H24	-	0.8	1
C4-H22	0.93	1.086	1.084	C4-C3-015	117.6	117.46	117.64	C2-C1-C7-O8	-12	167.9	163.2
C5-C6	1.364	1.391	1.387	C3-C4-C5	118.9	119.6	119.66	C2-C1-C7-O9	169	-13.6	-18.6
C5-H23	0.93	1.085	1.083	C3-C4-H22	121	118.2	118.94	C6-C1-C7-O8	167.6	-11.9	-16.5
C6-H24	0.93	1.084	1.082	C5-C4-H22	121	121.46	121.39	C6-C1-C7-O9	-10.6	166.5	161.4
C7-O8	1.228	1.217	1.209	C4-C5-C6	119.6	119.25	119.26	C1-C2-C3-C4	-0.7	2.5	2.5
C7-O9	1.3	1.357	1.356	C4-C5-H23	120	120.34	120.32	C1-C2-C3-015	175	177.3	177.4
O9-H10	0.93	0.973	0.969	C6-C5-H23	120	120.41	120.41	C11-C2-C3-C4	179.2	-176.1	-175.8
C11-H12	0.96	1.091	1.089	C1-C6-C5	121.8	121.04	121	C11-C2-C3-O15	-5.1	-1.39	-1
C11-H13	0.96	1.095	1.088	C1-C6-H24	119	118.03	118.12	C1-C2-C11-H12	-	-45.1	-42.2
C11-H14	0.96	1.09	1.093	C5-C6-H24	119	120.93	120.87	C1-C2-C11-H13	-	73.4	76.3
O15-C16	1.397	1.388	1.38	C1-C7-O8	121.3	123.96	124.09	C1-C2-C11-H14	-	-165.7	-162.8
C16-O17	1.1182	1.205	1.197	C1-C7-O9	114.8	115.1	114.52	C3-C2-C11-H12	-	133.4	135.9
C16-C18	1.469	1.512	1.51	O8-C7-H9	-	121.01	121.35	C3-C2-C11-H13	-	-108	-105.4
C18-H19	0.96	1.094	1.092	C7-O9-H10	112	106.07	106.34	C3-C2-C11-H14	-	12.8	15.3
C18-H20	0.96	1.094	1.092	C2-C11-H12	109	111.19	111.23	C2-C3-C4-C5	0.9	-1.7	-1.6
C18-H21	0.96	1.089	1.088	C2-C11-H13	109	111.46	111.4	C2-C3-C4-H22	-	177.4	177.4
				C2-C11-H14	109	110.3	110.24	O15-C3-C4-C5	-174.9	-176.5	-176.4
				H12-C11-H13	110	106.42	106.49	O15-C3-C4-H22	-	2.6	2.6
				H12-C11-H14	109	108.61	108.66	C2-C3-O15-C16	-	94.9	95.6
				H13-C11-H14	110	108.73	108.66	C4-C3-O15-C16	-	-89.9	-89.3
				C3-015-C16	119	122.31	122.35	C3-C4-C5-C6	-0.5	0.2	0.2
				O15-C16-017	121.6	117.86	117.93	C3-C4-C5-H23	-	179.9	179.8
				O15-C16-C18	112.1	117.56	117.3	H22-C4-C5-C6	-	-178.9	-178.8
				017-C16-C18	126.4	124.58	124.75	H22-C4-C5-H23	-	0.7	0.7
				C16-C18-H19	109	111.15	111.14	C4-C5-C6-C1	-0.2	0.2	0.1
				C16-C18-H20	109	110.97	110.83	C4-C5-C6-H24	-	179.9	179.7
				C16-C18-H21	109	108.08	108.13	H23-C5-C6-H24	-	0.2	0.1
				H19-C18-H20	110	107.22	107.23	C1-C7-O9-O10	-	-179	-179.1
				H19-C18-H21	110	109.83	109.89	O8-C7-O9-H10	0.8	0.5	-0.9

				H20-C18-H21	109	109.6	109.58	C3-O15-C16-O17	-	-179.7	179.5
								C3-O15-C16-C18	-	-0.3	-0.4
								O15-C16-C18-H19	-	-56.9	-56.1
								O15-C16-C18-H20	-	62.2	62.9
								O15-C16-C18-H21	-	-177.5	-176.8
								O17-C16-C18-H19	-	123	123.7
								O17-C16-C18-H20	-	-117.7	-117
								O17-C16-C18-H21	-	2.4	3

Table 2: Experimental and calculated (FT-IR and FT-Raman) frequencies (cm-1), IR intensity (KM mol-1), Raman activity (Å4 amu−1), force constants (m dyne Å-1), reduced mass (amu) and assignments for 3A2MBA

S No.	Experimental frequencies		Calculated with B3LYP/6-31+G(d,p)						Calculated with B3LYP/6-311++G(d,p)						Vibrational Assignments along with % of TED
	FT-IR	FT-Raman	Un scaled	Scaled	[a]IR int.	[b]Ra. act.	Force constants	Reduced mass	Un scaled	Scaled	[a]IR int.	[b]Ra. act.	Force constants	Reduced mass	
1.	3317vw		3752	3329	96.0305	151.12	8.8302	1.0643	3756	3322	99.8576	157.14	8.8508	1.0644	υO-H(100)
2.		3125w	3229	3136	2.8879	121.59	6.7212	1.0939	3209	3132	2.8469	123.19	6.6419	1.0942	υC-H (98)
3.		3100w	3212	3108	4.0237	141.16	6.6531	1.0945	3193	3105	3.2361	143.34	6.5753	1.094	υC-H(98)
4.		3075w	3198	3084	4.2768	63.26	6.5555	1.0879	3179	3081	3.4872	72.9	6.4804	1.0877	υC-H(99)
5.		2999w	3178	3006	6.091	76.73	6.5669	1.1032	3158	3002	7.2377	76.73	6.4833	1.1027	CH_3ops(96)
6.	2941w		3164	2953	5.4306	45.09	6.5093	1.103	3145	2949	5.0973	54.78	6.4305	1.1029	CH_3ops(96)
7.		2920w	3130	2928	2.8377	23.9	6.3523	1.1	3112	2926	2.9016	26.98	6.2756	1.0994	CH_3ss(95)
8.	2894w		3129	2902	8.5916	74.97	6.3037	1.0928	3111	2899	9.1109	83.78	6.2192	1.09	CH_3ss(95)
9.	2882w		3065	2894	2.5159	100	5.7437	1.0372	3053	2888	2.0183	98.89	5.6953	1.0368	CH_3ips(94)
10.		2868w	3062	2858	10.6401	87.22	5.7639	1.0431	3048	2854	9.366	87.22	5.7193	1.0446	CH_3ips(94)
11.	2847mw		1837	1976	445.4052	19	23.345	11.7311	1833	1971	457.7305	29.05	23.2448	11.7337	Rtrigd(56), bC–C(23)
12.		1769w	1781	1776	410.8519	82.68	18.1269	9.6993	1778	1773	428.2895	82.78	17.9724	9.647	υC=O(84)
13.	1763s		1643	1772	24.4671	54.84	9.9001	6.2183	1635	1769	22.315	56.8	9.7468	6.1827	υC=O(72)

14.	1694vs		1617	1702	22.9531	14.45	9.5189	6.1739	1610	1699	22.9094	14.68	9.301	6.0871	Rsymd(59), Rasymd(29), υC-C(19)
15.		1638mw	1506	1648	11.1238	5.53	1.5182	1.1357	1503	1645	10.7164	15.54	1.5096	1.334	υC-C(71), υC-H(16), bC- H(10)
16.	1623w		1502	1631	38.9715	4.63	2.0091	1.5108	1498	1627	36.3885	4.73	1.9393	1.4661	υC-C(65),bC-H(11), υC-H(13)
17.		1602ms	1486	1612	7.8827	3.84	2.3587	1.8109	1481	1608	8.7691	13.84	2.1665	1.6757	υC-C(69),bC-H(11),bC-C(14)
18.	1588w		1484	1595	23.5606	5.42	1.3876	1.0686	1480	1592	20.7156	6.42	1.4692	1.1382	υC-C(58), bC-H(15), ωC- O(15)
19.		1576mw	1475	1583	31.6921	2.91	2.3499	1.831	1471	1581	33.556	2.67	2.1437	1.6811	υC-C(59),ωC-H(15), bC-C(11)
20.	1482s		1468	1489	7.8665	6.65	1.4472	1.1394	1464	1487	7.8848	6.69	1.5141	1.1981	υC-C(54),bC-H(11),υC-C(6)
21.	1425ms		1425	1432	6.3769	11.26	1.4568	1.2173	1421	1429	6.4098	11.22	1.4493	1.218	CH_3ipb(89)
22.		1412ms	1403	1421	43.0211	1.37	1.4947	1.2881	1397	1418	38.7472	11.38	1.467	1.2744	CH_3ipb(89)
23.		1375w	1372	1384	122.7663	14.81	3.1331	2.8217	1364	1381	101.7417	14.87	2.8145	2.5664	bO-H(53), υC-C (18), bC-C(13)
24.	1364ms		1331	1371	18.1253	6.83	6.7414	6.4547	1316	1369	13.546	16.83	6.2122	6.0836	CH_3sb(63)
25.	1317s		1263	1324	70.0042	13.05	2.1158	2.2489	1259	1322	47.043	13.15	1.9958	2.1358	CH_3sb(63)
26.		1300w	1236	1305	122.5571	49.89	2.0635	2.2897	1234	1302	127.8708	47.89	2.663	2.5231	CH_3opb(54)
27.	1270ms		1219	1278	288.3423	7.03	2.719	3.1035	1213	1276	97.7131	17.03	2.1724	2.5024	CH_3opb(33)

28.		1262w	1207	1272	266.3554	9.39	2.1211	2.4704	1196	1268	377.9956	8.59	2.1041	2.4947	υC-O (46), υC-C (15), bC-O(11)
29.	1211vs		1190	1219	48.8286	7.5	1.2182	1.4577	1187	1217	129.4373	7.59	1.3292	1.5994	υC-O (46), υC-C (15), bC-O(11)
30.		1200ms	1141	1208	151.6279	6.24	2.108	2.7476	1133	1204	165.2799	17.23	2.2107	2.9199	υC-O (46), υC-C (15), bC-O(11)
31.	1129s		1102	1136	30.7544	12.95	1.4755	2.0619	1099	1134	34.8299	11.95	1.4816	2.0784	υC-C(59),ωC-H(15), bC-C(11)
32.		1087s	1062	1095	18.2063	0.66	1.1939	1.7957	1061	1092	8.9263	1.66	1.0941	1.6484	υC-C(54),bC-H(11),υC-C(6)
33.	1070ms		1060	1079	19.6232	2.14	1.1685	1.7648	1056	1077	27.4644	3.15	1.2587	1.9131	bC-H (71), bC-C(10), υC-O(13)
34.	1023s		1056	1035	9.6063	0.24	1.1351	1.7276	1055	1031	20.8739	0.26	1.1796	1.7967	bC-H (33), υC-O(13), bC-C(13)
35.	1011ms	996w	1008	1021	68.7894	1.68	1.0724	1.7887	1005	1018	63.2646	1.78	0.9956	1.6703	bC-H(60), bC-C(11), υC-O(10)
36.	936s		1000	949	1.3087	0.16	0.7852	1.3302	1002	946	25.6652	0.19	0.8714	1.4729	CH_3ipr(69)
37.	882mw		952	891	23.9304	2.84	1.6782	3.1416	950	889	6.1721	2.81	0.9744	1.8309	CH_3ipr(65)
38.		871w	949	845	5.6575	0.66	0.7538	1.4194	948	842	35.9437	1.66	1.1378	2.1477	CH_3opr(69)
39.	835mw		836	786	10.5158	2.55	1.1103	2.6942	837	784	7.7372	2.59	1.0998	2.6625	CH_3opr(65)
40.		807w	827	773	7.5315	3.77	1.3072	3.2387	827	771	7.8878	3.37	1.4487	3.5901	υC-C(44), bC-H(16), bC-O(11)

41.		781w	803	766	20.6397	2.39	1.9971	5.2506	801	764	28.5687	2.99	2.0267	5.356	ωC- H(24), υC-O(10),ωC- C(13)
42.	776mw		777	735	57.5217	0.29	1.0401	2.9172	778	734	51.5039	1.29	1.0264	2.8745	ωC- H(26), υC-O(8),ωC- C(10)
43.	764mw		730	713	10.4674	8.1	0.9081	2.889	732	711	11.6958	8.16	0.8378	2.6469	ωC- H(24), υC-O(16), ωC- C(8)
44.		756mw	702	663	9.102	13.62	1.0862	3.7366	705	660	9.9795	13.72	1.1699	3.9882	Rasymd(61), Rsymd(31), ωC-C(11)
45.	729w		651	632	46.5357	2.27	0.8042	3.2138	652	628	42.3604	2.37	1.0192	4.0668	bC-C(35), bC-O(13)
46.		704mw	627	621	95.3615	3.1	0.4099	1.7654	620	619	95.2087	3.17	0.3819	1.6824	ωO-H(22)
47.	654vw	615w	585	596	9.0229	7.35	1.0348	5.1153	586	594	9.4727	8.35	1.0057	4.968	bC-C(17), bO-C(21), bC-O(14),
48.	623w		567	574	8.1721	1.77	0.812	4.2813	570	571	9.5917	3.73	0.7044	3.6698	bC-C(13), bO-C(42)
49.		589w	564	553	1.9819	0.58	0.5152	2.744	566	549	1.8823	0.56	0.5135	2.7196	bC=O(13), ωC-C(11)
50.		564w	558	549	3.8108	2.26	0.6009	3.2681	555	546	5.1211	2.28	0.5871	3.2278	bC=O(32), bC-C(10)
51.	541w		497	537	0.5348	0.63	0.4658	3.1962	495	534	1.0079	0.53	0.457	3.153	bO-C(16), bC-C(48)
52.		538w	464	521	3.4745	0.21	0.4804	3.7812	465	518	3.8813	0.27	0.4831	3.7836	bO-C(20),υC-O(16), ωC-C (13)
53.	529w		414	461	0.6312	1.91	0.6299	0.2218	413	459	0.5864	1.9	0.6167	6.1226	bC-O(32), bC-C(12), υC- C(10)

54.		512w	390	455	4.4975	2.79	0.6395	7.1072	390	451	3.9782	2.39	0.6035	6.7057	tRtring(57), tRasymd(17),ωC-C(08)
55.	454vw		366	419	3.1834	1.48	0.2948	3.7213	365	415	3.881	1.44	0.2904	3.6948	ωC- C(22),bO-H(16)
56.	447vw		340	303	3.1008	4.34	0.375	5.4994	340	299	2.7744	4.36	0.3778	5.5446	ωC- C(17), ωO-C (27)
57.	432s		303	279	5.2793	1.91	0.2189	4.0336	301	275	5.6777	1.61	0.2163	4.05	ωC=O(20),υC-O(16), ωC-C (13)
58.	424w		230	253	2.6287	0.03	0.175	5.5985	227	249	2.4486	0.23	0.1736	5.6761	ωC-C(24), bC-O(10), ωC-C(20)
59.	418w		210	241	1.4552	1.64	0.0945	3.6221	207	237	1.6139	1.67	0.0919	3.6246	ωC=O(18),υC-O(16), ωC-C (13)
60.		412w	182	216	0.0686	0.57	0.022	1.1212	171	212	0.0496	0.97	0.0192	1.114	ωO-C(19),υC-O(16), ωC-C (13)
61.		294ms	139	137	0.4512	0.54	0.0178	1.5609	137	134	0.7568	0.58	0.0204	1.8452	ωO-C(20),υC-O(08), ωC-C (13)
62.		230w	132	112	0.7432	1.04	0.0192	1.8516	129	109	0.6526	1.34	0.0157	1.5815	ωO-C(20),υC-O(16), ωC-C (13)
63.		142w	73	84	0.7816	1.07	0.0131	4.1042	73	81	0.714	1.97	0.0127	3.9753	tRsymd(51), tRtring(33), bC-C(10)
64.		127s	57	76	6.1756	1.83	0.0091	4.6943	56	72	5.985	1.87	0.0084	4.4099	tRasymd(61), tRsymd(27),υC-C(11)

65.		101vs	42	63	1.3241	2.16	0.0057	5.4214	41	61	1.7806	2.19	0.0066	6.6502	τCH_3 (69)
66.		75vs	31	57	1.9438	0.75	0.0048	7.9395	34	54	1.2109	0.89	0.0051	7.2246	τCH_3 (55)

[a]IR intensity. [b]Raman activity

Abbreviations: vs: very strong; ms: medium strong; s: strong; w: weak; mw: medium weak; vw: very weak; ips: inplane stretching; ops: out-of-plane stretching; ss: symmetric stretching; ipb: in-plane bending; opb: out-of-plane bending; sb: stretching bending; τ: twisting.

Methyl Group Vibrations

The 3A2MBA molecule consists of two CH_3 groups, one unit in benzene ring and another in the acetoxy group, which lies in the tertiary position of the molecule. For the assignments of CH_3 group frequencies, nine fundamentals can be associated to each CH_3 group[53] namely CH_3ss–symmetric stretch; CH_3ips–in-plane stretch (i.e. in-plane hydrogen stretching modes); CH_3ipb- in-plane bending (i.e. in-plane hydrogen deformation modes); CH_3sb–symmetric bending; CH_3ipr–in-plane rocking; CH_3ops–out-of-plane stretching; CH_3opb-out-of-plane bending; CH_3opr–out-of-plane rocking and τCH_3–torsion. The C–H stretching in CH_3 occurs at lower frequencies than those of aromatic ring. Moreover, the asymmetric stretch is usually at higher wavenumber than the symmetric stretch. Methyl group vibrations are generally referred to as electron-donating substituent in the aromatic rings system. Acetoxy group comprises a methyl and an ester group. The hydrogen in the methyl group acts as an electron donor, whereas oxygen present in the ester is an electron acceptor. The anti-symmetric and symmetric stretching vibrations are in the ranges 3050-2950 and 2970-2860 cm^{-1} [54]. In the present study, two CH_3 anti symmetric stretching vibrations are observed at 2999 and 2941 cm^{-1} in FT-Raman and FT-IR respectively. Two CH_3 symmetric stretching modes are observed as weak bands in FT-IR and FT-Raman spectra at 2894 and 2920 cm^{-1} of title molecule and the corresponding two CH_3ips, in-plane stretching modes are observed in FT-IR spectrum at 2882 and 2847 cm^{-1}. The CH_3 asymmetric and symmetric stretching vibrations predicted theoretically by B3LYP/6-311++G (d,p) method show excellent agreement with the experimental values. It shows above 90% of TED contribution suggesting that it is pure stretching mode. For methyl substituted benzene derivatives the antisymmetric and symmetric deformation vibrations of methyl group normally appear in the regions 1480-1410 and 1385-1250 cm^{-1} [54,55] respectively. In the FT-IR and FT-Raman spectra, the bands occurred at 1425, 1364, 1317, 1270 and 1412, 1300 cm^{-1} are due to antisymmetric and symmetric deformations. The computed values are predicted by B3LYP/6-31+G (d,p) and 6-311++G (d,p) method show good agreement with literature as well as experimental observations. The rocking vibrations of CH_3 modes usually appear in the region 1070-826 cm^{-1} [56]. The Strong and medium weak bands observed at 936 and 882 cm^{-1} in FT-IR Spectrum are assigned to two CH_3ipr– in-plane rocking vibrations and its counterpart, CH_3opr–out-of-plane rocking vibrations were observed at 871 and 835 cm^{-1} in FT-Raman and FT-IR spectra. The experimental and theoretically wavenumbers are predicted of CH_3 rocking vibrations show good correlation with the literature data of the title molecule. The CH_3 torsional modes of vibrations were assigned in the lower region of the Raman spectrum and the values are in line with the theoretical values.

Molecular Orbital Studies

The most widely used theory by chemists is the molecular orbital (MO) theory. It is important that Ionization Potential (IP), Electron Affinity (EA), Electrophilicity Index (ω), Chemical Potential (μ), Electronegativity (χ) and Hardness (η) be put into a MO framework. These are readily being done within the limitations of Koopman′s theorem the orbital energies of the frontier orbital are given by Figure 4 show an orbital energy diagram for 3A2MBA molecule. Only the HOMO and LUMO orbitals are shown. On the basis of a fully optimized ground state structure, the DFT/B3LYP/6-31+G(d,p) and 6-311++G(d,p) calculations predicts one intense electronic transition from the ground to the first excited state and is mainly described by one electron excitation from the highest occupied molecular orbital (HOMO) to the lowest unoccupied molecular orbital (LUMO). We focus on the HOMO and LUMO energies in order to determine interesting molecular/atomic properties and chemical quantities. In simple molecular orbital theory approaches, the HOMO energy (HOMO) is related to the IP by Koopmans's theorem and the LUMO energy (LUMO) has been used to estimate the electron affinity (EA) [57]. If HOMO and LUMO, then the average value of the HOMO and LUMO energies is related to the electronegativity (χ) defined by Mulliken [58] with χ = (IP +A)/2. In addition, the HOMO-LUMO gap is related to the hardness (η) [59-62], and also Parr et al. [57] defined global electrophilicity as a quantitative intrinsic numerical value and suggested the term electrophilicity index (ω), a new global reactivity descriptor of molecule, as $=\mu^2/2$ where μ is the chemical potential takes the average value [61] i.e., μ = (IP +EA)/2. In general, the electrophiles are electron lovers or electron deficient and hence prefer to accept electrons and form bonds with nucleophiles. Thus electrophilicity is useful structural depictor of reactivity and is frequently used in the analysis of the chemical reactivity of molecule [62]. The title molecule with low potential is a good electrophile; an extremely hard molecule has feeble electron acceptability. Consequently, a measure of molecular electrophilicity depends on both the chemical potential and the chemical hardness. Finally, the calculated HOMO-LUMO gaps are also closer to the first electronic excitation energies. The electronegativity and hardness are of course used extensively to make predictions about chemical behavior and these are used to explain aromaticity in organic compounds [62]. A hard molecule has a large HOMO-LUMO gap and a soft molecule has a small HOMO-LUMO gap. In quantum theory, changes in the electron density of a chemical system result from the mixing of suitable excited-state wave function with the ground state wave function. The mixing coefficient is inversely proportional to the excitation energy between the ground and excited state. A small HOMO-LUMO gap automatically means small excitation energies to the manifold of

excited states. Therefore, soft molecule, with a small gap, will have their electron density changed more easily than a hard molecule. In terms of chemical reactivity, we can conclude that soft molecule will be more reactive than hard molecule. The HOMO is located over methyl group atoms and acetoxy group atoms, and the HOMO-LUMO transition implies an electron density transfer to the carboxylic group. Moreover, these orbitals significantly overlap in their position for 3A2MBA is shown in Figure 4. The HOMO-LUMO energy gap of 3A2MBA were calculated at the B3LYP/6-31+G(d,p) and 6-311++G(d,p) levels, which reveals that the energy gap reflects the chemical activity of the molecule. The LUMO as an electron acceptor represents the ability to obtain an electron and HOMO represents the ability to donate an electron. The energy gap between the HOMO and the LUMO molecular orbitals is a critical parameter in determining molecular electrical transport properties because it is a measure of electron conductivity. The energy gap values of HOMO-LUMO are -4.09151 and -5.23710 eV of 3A2MBA, respectively. Lower value in the HOMO and LUMO energy gap explains the eventual charge transfer interactions taking place within the molecule. The calculated chemical hardness, softness, chemical potential, electrophilicity, ionization potential, electron affinity and electronegativity are presented in Table 3.

Natural Atomic Orbitals

The occupancies and energies of bonding molecular orbitals of the title molecule is predicted at B3LYP/6-311++G (d,p) level of theory and presented in Table 4. The variations in occupancies and energies of 3A2MBA directly give the evidence for the delocalization of charge upon substitution and this leads to the variation of bond lengths of the title molecule as shown in Table 1.

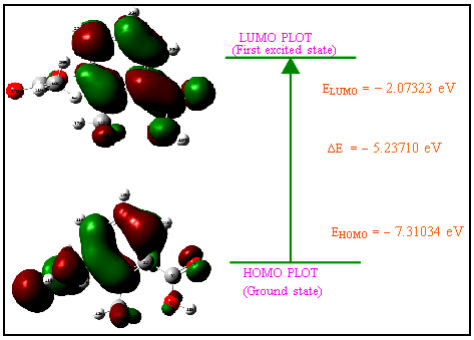

Figure 4: The atomic orbital compositions of the frontier molecular orbital for 3A2MBA along with B3LYP/ 6-311++G (d,p) method basis set

Table 3: Calculated molecular properties of 3A2MBA from orbital energies

Chemical parameters(in eV)	Values of B3LYP	
	6-31+G(d,p)	6-311+G(d,p)
E_{HOMO}	-9.4195	-7.31034
E_{LUMO}	-5.32799	-2.07323
Energy gap	-4.09151	-5.2371
Ionization potential (I)	9.4195	7.31034
Electron affinity (A)	5.32799	2.07323
Electronegativity(c)	7.37374	4.69179
Global hardness (h)	2.04575	2.61856
Chemical potential (μ)	-7.37374	-4.691789
Global Electrophilicity (ω)	13.28895	4.20334
Softness(S)	361.94993	282.7743

Table 4: Comparison of occupancies and energies of bonding molecular orbitals for 3A2MBA using B3LYP/6-311++G (d,p) method

Atomic orbitals[a]	Occupancies(e)	Energies(a.u)
BD(C1-C2)	1.97273	-0.7197
BD(C1-C6)	1.97246	-0.71329
BD(C1-C7)	1.97302	-0.65816
BD(C2-C3)	1.95601	-0.71169
BD(C2-C11)	1.97904	-0.61442
BD(C3-C4)	1.96243	-0.70936
BD(C3-O15)	1.98627	-1.36283
BD(C4-C5)	1.98051	-0.70994
BD(C4-H22)	1.97952	-0.54334
BD(C5-C6)	1.97749	-0.70788
BD(C5-H23)	1.98053	-0.53596
BD(C6-H24)	1.9783	-0.52809
BD(C7-O8)	1.99618	-1.06411
BD(C7-O9)	1.99549	-0.94929
BD(O9-H10)	1.98673	-0.77435

BD(C11-H12)	1.97635	-0.51312
BD(C11-H13)	1.97711	-0.51607
BD(C11-H14)	1.98875	-0.81925
BD(O15-C16)	1.93138	-1.0999
BD(C16-O17)	1.99622	-0.67934
BD(C16-C18)	1.9848	-0.67934
BD(C18-H19)	1.96713	-0.55508
BD(C18-H20)	1.97168	-0.55207
BD(C18-H21)	1.98172	-0.54941

Natural Population Analysis

The natural population analysis [63] performed on the electronic structure of 3A2MBA clearly describes the distribution of electrons in various sub-shells of their atomic orbitals. The accumulation of charges on the individual atom and the accumulation of electrons in the core, valence and Rydberg sub-shells are also presented in Table 5. In the case of 3A2MBA, the most electropositive charge of 0.80034e is accumulated on C7 and 0.779092e is accumulated on C16 atom. According to an electrostatic point of view of the molecule, these electropositive atoms have a tendency to accept an electron. Whereas, the most electronegative atoms such as; O15 (-0.46472e), O17 (-0.52325e), O8 (-0.60688e) and O9 (-0.70951e) have a tendency to donate an electron. The substituent effect may cause a change in the magnitude of these charges observed in 3A2MBA. In view of title molecule, the electronegative atoms O8, O9, O15 and O17 are of variations in magnitude of natural charges on C7 and C16 of electropositive atoms. Further, the natural population analysis showed that 102 electrons in the 3A2MBA molecule are distributed on the sub-shells as follows:

Core: 27.98971 (99.9633% of 28); Valence: 73.67036 (99.5545% of 74); Rydberg: 0.33993 (0.3333% of 102).

Table 5: Accumulation of natural charges, population of electrons in core, valence and Rydberg orbitals of 3A2MBA using B3LYP/6-311++G (d,p) method

Atom	Charges (e)	Natural population(e)			Total (e)
		Core	Valence	Rydberg	
C1	-0.15182	1.99877	4.13422	0.01884	6.15182
C2	-0.02726	1.99896	4.00977	0.01853	6.02726
C3	0.28526	1.99884	3.67513	0.04076	5.71474
C4	-0.23409	1.99914	4.21801	0.01695	6.23409
C5	-0.19309	1.99921	4.17679	0.01708	6.19309
C6	-0.18491	1.99909	4.1679	0.01792	6.18491
C7	0.80034	1.99944	3.15158	0.04864	5.19966
O8	-0.60688	1.99976	6.59455	0.01257	8.60688
O9	-0.70951	1.99975	6.69587	0.01389	8.70951
H10	0.49756	0	0.49849	0.00396	0.50244
C11	-0.59846	1.99927	4.58713	0.01207	6.59846
H12	0.23382	0	0.7648	0.00138	0.76618
H13	0.22003	0	0.77845	0.00152	0.77997
H14	0.19643	0	0.80208	0.00149	0.80357
O15	-0.46472	1.99921	6.43312	0.03239	8.46472
C16	0.77909	1.99936	3.16952	0.05204	5.22091
O17	-0.52325	1.99975	6.51103	0.01248	8.52325
C18	-0.68548	1.99917	4.67778	0.00853	6.68548
H19	0.23819	0	0.76043	0.00138	0.76181
H20	0.24442	0	0.75409	0.00149	0.75558
H21	0.23974	0	0.75918	0.00108	0.76026
H22	0.2102	0	0.78808	0.00173	0.7898
H23	0.20855	0	0.79003	0.00142	0.79145
H24	0.22584	0	0.77236	0.0018	0.77416

Natural Bond Orbital Analysis

The information about the charge delocalization and the chemical reactivity is being helpful to the drug designers to design new type of drugs. The natural bond orbital (NBO) is an effective tool for the elucidation of residual resonance delocalization effects of a molecule and it also illustrates the deciphering of the molecular wave function in terms of Lewis structures, charge, bond order, bond type, hybridization, resonance, donor-acceptor interactions, etc. [64]. Therefore, the NBO analysis of certain pharmaceutical compounds has been performed by various spectroscopists [65-70]. The natural bond orbital (NBO) analysis of 3A2MBA molecule is being performed at DFT/B3LYP/6-311+G level to estimate the delocalization patterns of electron density (ED) from the principle occupied Lewis-type (bond or lone pair) orbitals to unoccupied non-Lewis (anti-bonding or Rydberg) orbitals. Table 6 lists the occupancies and energies of most interacting NBO's along with their percentage of hybrid atomic orbital [71] contribution. The percentage of hybrid atomic orbitals of oxygen lone pair atoms O8, O9, O15 and O17 of 3A2MBA showed that they are partially contributed to both *s*-type and *p*-

type sub-shells. In contrast, all the anti-bonding orbitals of 3A2MBA are mainly contributed to *p*-type sub-shell. The interactions result in a loss of occupancy from the localized NBO of the idealized Lewis structure into an empty Non-Lewis orbital. For each donor (*i*) and acceptor (*j*), the stabilization energy, $E^{(2)}$ associated with the delocalization *i j* is estimated as:

$$E^{(2)} = \Delta E_{ij} = q_i \frac{F(i,j)}{\varepsilon_j - \varepsilon_i} \quad \text{... (2)}$$

Where q_i is the donor orbital occupancy, ε_i and ε_j are diagonal elements and $F(i,j)$ is the off diagonal NBO Fock matrix element. The NBO analysis provides an efficient method for studying intra-and intermolecular bonding hyperconjugative interactions of π electrons and also provides a convenient basis for investigating charge transfer or conjugative interactions in molecular systems [72]. The transferring of energy during the intermolecular interactions between LP (2) O (9) and π^*(C7-O8) bond is more, which is about 44.79 kj/mol for 3A2MBA. The maximum energy delocalization takes part in the $\pi^* \rightarrow \pi^*$ transition. In 3A2MBA, the intra molecular hyper conjugative interaction of the σ(C1–C2) and π (C1-C2) are distributed to σ^*(C3-O15) → 4.41 kj/mol and π^* (C3-C4)→ 19.15kj/mol, π^* (C5-C6)→ 20.81 kj/mol, π^* (C7-O8)→ 20.77 kj/mol. Whereas π^*(C7-O8), π^* (C3-C4) and π^*(C1-C2), π^*(C5-C6) bonds are more, which is about 105.33 and 233.77 kj/mol for 3A2MBA at ground state. The $E^{(2)}$ values and types of the transition is shown in Table 6.

Table 6: Second order perturbation theory analysis of fock matrix in NBO basis for 3A2MBA using B3LYP/6-311++G(d,p) method

Donor(i)	Acceptor(j)	E(2)[a] (kj mol^{-1})	E(j) -E(i)[b] ×10^3(kj mol^{-1})	F(i,j)[c] ×10^3(kj mol^{-1})
σ (C1-C2)	σ^* (C3-O15)	4.41	1.02	0.06
σ (C3-C4)	σ^* (C2-C3)	3.61	1.27	0.061
π (C1-C2)	π^* (C3-C4)	19.15	0.27	0.065
	π^* (C5-C6)	20.81	0.28	0.07
	π^* (C7-O8)	20.77	0.26	0.067
π (C3-C4)	π^* (C1-C2)	21.38	0.29	0.071
		17.01	0.3	0.064
π (C5-C6)	π^* (C1-C2)	18.51	0.28	0.064
	π^* (C3-C4)	22.71	0.27	0.07
LP(2) O9	π^* (C7-O8)	44.79	0.34	0.113
LP(2) O15	π^*(C16-O17)	40.18	0.34	0.104
LP(2) O17	π^*(O15-C16)	37.13	0.59	0.133
	π^*(C16-C18)	18.33	0.62	0.098
π^* (C3-C4)	π^* (C5-C6)	233.77	0.01	0.081
π^* (C7-O8)	π^* (C1-C2)	105.33	0.02	0.072

[a] $E^{(2)}$ means energy of hyper conjugative interactions (stabilization energy); [b] Energy difference between donor and acceptor i and j NBO orbitals; [c] F(i, j) is the Fock matrix element between i and j NBO orbitals

Thermodynamic Properties

The computation of vibrational frequencies simultaneously leads to prediction of several thermodynamic properties too. The equations utilized for computing thermochemical data in Gaussian programs are derived from statistical thermodynamics with the two key ideas, the Boltzmann distribution and the partition function. Several calculated thermodynamic parameters are presented in prediction in Table 7.

Table 7: The calculated thermodynamic parameters of 3A2MBA

Thermodynamic properties	B3LYP	
	6-31+G(d,p)	6-311++G(d,p)
SCF energy	-691.0405882	-688.0303882
Zero-point vibrational energy (kcal/mol)	116.85996	115.39713
Rotational temperature (K)		
A	0.06473	0.06472
B	0.02375	0.02073
C	0.01955	0.01725
Rotational constants (GHz)		
A	1.34867	1.34853
B	0.4948	0.4319
C	0.40741	0.35942
Dipole moment (Debye)		
μ_x	0.0574	0.0574
μ_y	-0.5519	-0.5519
μ_z	1.1273	1.1273
μ_{Total}		1.2565
Total entropy (cal/mol/K)	100.511	117.285
Translational	41.694	41.694

Rotational	31.448	31.707
Vibrational	27.369	43.884
Total heat capacity at constant volume (cal/mol/K)	42.776	49.119
Translational	2.981	2.981
Rotational	2.981	2.981
Vibrational	36.814	43.157
Total thermal energy (kcal/mol)	123.502	123.782
Translational	0.889	0.889
Rotational	0.889	0.889
Vibrational	121.724	122.005
Thermal corrections (Hartree/Particle)		
Zero-point	0.186228	0.183897
Energy	0.196812	0.197259
Enthalpy	0.197756	0.198204
Gibbs free energy	0.15	0.142478
Sum of thermal corrections and energy (Hartree)		
Zero-point energies	-687.84416	-688.021722
Thermal energies	-687.833576	-688.008359
Thermal enthalpy	-687.832632	-688.007415
Thermal free energy	-687.880388	-688.063141

Scale factors have been recommended for an accurate determining the zero-point vibration energies (ZPVE), rotational constants, thermal energy and the entropy of the 3A2MBA was directly obtained from the output of Gaussian programs in the optimization and vibration calculations. These attributes includes such as enthalpy (H_m^o), entropy (S_m^o), heat capacity at constant volume (C_v) and pressure (C_p) which are contributed by translational, rotational and vibrational partition functions [73]. In addition, SCF energy, zero point vibrational energy, total thermal energy, rotational constants, thermal corrections and dipole moment in all the three dimensions of space were calculated and given in Table 7 for 3A2MBA under B3LYP/6-31+G(d,p) and B3LYP/6-311++G(d,p) model chemistry. All these thermodynamic data provide helpful information on further study of this title molecule, while using as reactant to take part in a new reaction, chemical physics analysis as well as to propose organic reaction mechanisms. These standard thermodynamic functions can be used as reference thermodynamic values to calculate changes which take place in entropy, Gibbs free energy, internal energy, heat capacity and enthalpy of 3A2MBA in its organic chemical transformation [74,75].

CONCLUSION

A complete vibrational analysis of 3-acetoxy-2-methylbenzoic acid was performed based on calculation at the B3LYP/6-31+G(d,p) and 6-311++G(d,p) levels. The theoretical results were compared with the experimental vibrations. Scaling factors results are in good agreement with the experimental values. The computed geometrical parameters are in good agreement with the literature values of this compound. The influences of acetoxy and methyl groups to the vibrational frequencies were also discussed. Natural atomic orbitals, natural population analysis and natural bond orbital analysis are determined. Other electronic structure properties such as chemical hardness, chemical potential, electrophilicity, ionization potential, electron affinity, electronegativity and HOMO-LUMO analysis of the molecule have been calculated. The entire calculated quantum chemical investigations can lay a strong foundation for 3A2MBA to extend its application in organic chemical transformation, material sciences and to model potential bioactive targets.

REFERENCES

[1] P Mani. Thesis, Pondicherry University, **2004**, 107.
[2] SK Sagoo; R Board; S Roller. *Lett Appl Microbiol*. **2002**, 34(3), 168-172.
[3] H Haque; TJ Cutright; BMZ Newby. *Biofoul*. **2005**, 21, 109-119.
[4] G Bruno; L Randaccio. *Acta Cryst*. **1980**, 36B, 1711-1712.
[5] CC Wilson; N Shankland; AJ Florence. *J Chem Soc Faraday Trans*. **1996**, 92, 5051-5057.
[6] J Krausse; H Dunken. *Acta Cryst*. **1966**, 20, 67-73.
[7] G Ferguson; GA Sim. *Acta Cryst*. **1961**, 14, 1262-1270.
[8] M Polito; E D'Oria; L Maini; PG Karamertzanis; F Grepioni; D Braga; SL Price. *Cryst Eng Comm.* **2008**, 10, 1848-1854.
[9] G Chiari; FR Fronczek; ST Davis; RD Gandour. *Acta Cryst*. **1981**, B37, 1623-1625.
[10] FR Fronczek; ML Merrill; RD Gandour. *Acta Cryst*. **1982**, B38, 1337-1339.
[11] B Roland; L Lazzarato; M Donnolo; Elizabeth. *Chem Med Chem*. **2013**, 8(7), 1199-1209.
[12] U Derhaschnig; IS Exeli; C Marsik; F Cardona; P Minuz; B Jilma. *Platelets.* **2010**, 21, 320328.

[13] VK Rastogi; MP Rajpoot; SN Sharma. *Ind J Phys*. **1984**, 58B, 311-314.
[14] S Ahamed; S Mathew; PK Verma. *Ind J Phys*. **1992**, 30, 764-765.
[15] M Chaman; PK Verma. *Ind J Phys*. **2003**, 77B (3), 315-318.
[16] N Sundaraganesan; BD Joshua; T Radjakoumar. *Ind J Pure Appl Phys*. **2009**, 47, 248-258.
[17] N Sundaraganesan; BD Joshua; K Settu. *Spectrochim Acta*. **2007**, 66A, 381-388.
[18] N Sundaraganesan; S Ilakiamani; BD Joshua. *Spectrochim Acta*. **2007**, 66A, 287-297.
[19] M Amalanathan; VK Rastogi; I Hubert Joe. *Spectrochim Acta Part A*. **2011**, 78(5), 1437-1444.
[20] R Cosmo; A Dierdorf. Inventors; Clariant GmbH, assignee. Process for the preparation of 3-hydroxy-2-methylbenzoic acid and 3-acetoxy-2-methylbenzoic. United States patent US 5,910,605. **1999**.
[21] M Saranya; A Subashini; C Arunagiri; PT Muthiah. *Acta Cryst*. **2015**, E71, 474.
[22] HG Korth; MI de Heer; P Mulder. *J Phys Chem*. **2002**, 106, 8779-8789.
[23] R Karmakar; A Samanta. *J Phys Chem*. 2003, 107A, 7340-7346.
[24] V Chis. Chem Phys. **2004**, 300, 1-11.
[25] N Kobko; JJ Dannenberg. *J Phys Chem*. **2003**, 107A, 10389-10395.
[26] Gaussian 09W Program, *Gaussian Inc*, Wallingford, CT, **2009**.
[27] D Becke. J Chem Phys. **1993**, 98, 5648-5652.
[28] A Lee; W Yang; RG Parr. *Phys Rev*. **1998**, 37B, 785-789.
[29] V Krishanakumar; S Dheivamalar. *J Raman Spectro*. **2009**, 40, 411-415.
[30] P Pulary; G Fogarasi; G Pongor; JE Bogg; A Vargha. *J Am Chem Soc*. **1983**, 105, 7073-7047.
[31] G Rauhut; P Pulay. J Phys Chem. **1995**, 99, 3093-3100.
[32] G Fogarasi; X Zhou; PW Taylor; P Pulay. *J Am Chem Soc*. **1992**, 14, 8191-8201.
[33] T Sundius. *J Mol Struct*. **1990**, 218, 321-326.
[34] T Sundius. QCPE Program. **2002**, 807.
[35] T Sundius. *Vib Spectrosc*. **2002**, 29, 89-95.
[36] N Sundaraganesan; B Dominic Joshua; C Meganathan; R Meenashi; JP Cornard. *Spectrochim Acta A.* 70, **2008**, 376-383.
[37] G Varsanyi. Vibrational Spectra of Benzene Derivative, Academic Press, New York, **1969**.
[38] RM Silverstein, FX Webster. Spectroscopic Identification of Organic Compound, 6th edition, John Willey & Sons, New York, **1998**.
[39] B Smith. Infrared Spectral Interpretation, A Systematic Approach, CRC Press, Washington DC, **1999**.
[40] C Arunagiri; A Subashini; M Saranya; P Thomas Muthiah; K Thanigaimani; A Razak. *Spectrochim Acta*. **2015**, 307-316.
[41] FR Dollish, WG Fateley, FF Bentley. Characteristic Raman Frequencies of Organic Compounds, John Wiley & Sons, New York, **1997**.
[42] M Cinar; N Yildiz; M Karabacak; M Kurt. *Spectrochim Acta*, 105A, **2013**, 80-87.
[43] M Karabacak; Z Cinar; M Kurt; S Sudha; N Sundaraganesan. *Spectrochim Acta Part A85.* **2012**, 179-189.
[44] G Varsanyi. Assignments for Vibrational Spectra of Seven Hundred Benzene Derivatives, Academia Kiado, Budapest, **1973**.
[45] S Bayari; S Saglam; HF Ustundag. *J Mol Struct*. 726, **2005**, 225-232.
[46] A Srivastava; VB Singh. *Indian J Pure Appl Phys*. 2007, 45, 714-720.
[47] N Sundaraganesan; S Illakiamani; H Saleem; PM Wojciechowski; D Michalska. *Spectrochim Acta*. **2005**, 61A, 2995-3001.
[48] D Lin-Vien, NB Colthup, WG Fateley, JG Grasselli. The Hand book of Infrared Raman Characteristic Frequencies of Organic Molecules, Academic Press, Boston, MA, **1991**.
[49] S Sebastain; N Sundaraganesan; S Manoharan. *Spectrochim Acta74 A.* **2009**, 312-323.
[50] K Nakamoto. Infrared and Raman Spectra of Inorganic and Coordination Compounds, 6th edition, John Wiley & Sons Inc, Hoboken, New Jersey, **2009**.
[51] B Venkatram Reddy; G Ramana Rao. *Vib Spectrosc*. **1994**, 6, 259-265.
[52] JF Arenas; I Lopez Tocon; JC Otero; JI Marcos. *J Mol Struct.* **1997**, 410, 443-446.
[53] DA Long; WO Jeorge. *Spectrochim Acta.* **1963**, 19, 1777-1799.
[54] P Politzer; F Abu-Awwad. *Theor Chem Acta.* **1998**, 99, 83-87.
[55] RS Mulliken. *J Chem Phys*. **1934**, 2, 782-793.
[56] RG Parr; RG Pearso. *J Am Chem Soc*. **1983**, 105, 7512-7516.
[57] RG Parr, W Yang. Density Functional Theory for Atoms and Molecules, Oxford University Press, New York, **1982**.
[58] RG Pearson. Chemical hardness, JohnWiley-VCH, Weinheim, **1997**.
[59] RG Parr; LV Szentpaly; S Liu. *J Am Chem Soc*. **1999**, 121, 1922-1924.
[60] J Padmanabhan; R Parthasarathi; V Subramanian; PK Chattaraj. *J Phys Chem*. **2007**, 111A, 1358-1361.
[61] PK Chattaraj; B Maiti; U Sarkar. *J Phys Chem*. **2003**, 107A, 4973-4975.

[62] F De Proft; P Geerlings. *Chem Rev*. **2001**, 101, 1451-1464.
[63] E Reed; RB Weinstock; F Weinhold. *J Chem Phys*. **1985**, 83, 735-746.
[64] ED Glendening; CR Landis; F Weinhold. *WIREs Comput Mol Sci*. **2012**, 2, 1-42.
[65] JD Magdaline; T Chithambarathanu. Indian *J Pure Appl Phys*. **2012**, 50, 7-13.
[66] ZR Zhou; LX Hong; ZX Zhou. *Indian J Pure Appl Phys*. **2012**, 50, 719-726.
[67] T Karthick; V Balachandran; S Perumal; A Natraj. *J Mol Struct*. **2011**, 1005, 192-201.
[68] LX Hong; ZR Zhou; ZX Zhou. *Indian J Pure Appl Phys*. **2012**, 50, 697-705.
[69] V Balachandran; T Karthick; S Perumal; A Natraj. *Spectrochim Acta*. **2012**, 92A, 137-147.
[70] S Chandra; H Saleem; S Sebastian; N Sundaraganesan. *Spectrochim Acta*. **2011**, 78A, 1515-1524.
[71] JP Foster; F Weinhold. *J Am Chem Soc*. **1980**, 102, 7211-7218.
[72] L Sinha; M Karabacak; V Narayan. M Cinar; O Prasad. *Spectrochim Acta*. **2013**, 298-307.
[73] DA McQuarrie; JD Simon. Nonequilibrium thermodynamics. Molecular Thermodynamics. University Science Books, Sausalito, CA. **1999**, 581-627.
[74] D Sajan; L Joseph; N Vijayan; M Karabacak. *Spectrochim Acta.* 2011, 81A, 85-9.